The NEW ENGLAND JOURNAL of MEDICINE

ESTABLISHED IN 1812 OCTOBER 7, 2010 VOL. 363 NO. 15

Patient-Specific Induced Pluripotent Stem-Cell Models for Long-QT Syndrome

Alessandra Moretti, Ph.D., Milena Bellin, Ph.D., Andrea Welling, Ph.D., Christian Billy Jung, M.Sc., Jason T. Lam, Ph.D., Lorenz Bott-Flügel, M.D., Tatjana Dorn, Ph.D., Alexander Goedel, M.D., Christian Höhnke, M.D., Franz Hofmann, M.D., Melchior Seyfarth, M.D., Daniel Sinnecker, M.D., Albert Schömig, M.D., and Karl-Ludwig Laugwitz, M.D.

ABSTRACT

BACKGROUND

Long-QT syndromes are heritable diseases associated with prolongation of the QT interval on an electrocardiogram and a high risk of sudden cardiac death due to ventricular tachyarrhythmia. In long-QT syndrome type 1, mutations occur in the *KCNQ1* gene, which encodes the repolarizing potassium channel mediating the delayed rectifier I_{Ks} current.

METHODS

We screened a family affected by long-QT syndrome type 1 and identified an autosomal dominant missense mutation (R190Q) in the *KCNQ1* gene. We obtained dermal fibroblasts from two family members and two healthy controls and infected them with retroviral vectors encoding the human transcription factors OCT3/4, SOX2, KLF4, and c-MYC to generate pluripotent stem cells. With the use of a specific protocol, these cells were then directed to differentiate into cardiac myocytes.

RESULTS

Induced pluripotent stem cells maintained the disease genotype of long-QT syndrome type 1 and generated functional myocytes. Individual cells showed a "ventricular," "atrial," or "nodal" phenotype, as evidenced by the expression of cell-type–specific markers and as seen in recordings of the action potentials in single cells. The duration of the action potential was markedly prolonged in "ventricular" and "atrial" cells derived from patients with long-QT syndrome type 1, as compared with cells from control subjects. Further characterization of the role of the R190Q–KCNQ1 mutation in the pathogenesis of long-QT syndrome type 1 revealed a dominant negative trafficking defect associated with a 70 to 80% reduction in I_{Ks} current and altered channel activation and deactivation properties. Moreover, we showed that myocytes derived from patients with long-QT syndrome type 1 had an increased susceptibility to catecholamine-induced tachyarrhythmia and that beta-blockade attenuated this phenotype.

CONCLUSIONS

We generated patient-specific pluripotent stem cells from members of a family affected by long-QT syndrome type 1 and induced them to differentiate into functional cardiac myocytes. The patient-derived cells recapitulated the electrophysiological features of the disorder. (Funded by the European Research Council and others.)

From the Cardiology Division, First Department of Medicine (A.M., M.B., C.B.J., J.T.L., L.B.-F., T.D., A.G., M.S., D.S., A.S., K.-L.L.), and the Plastic Surgery Department (C.H.), Klinikum rechts der Isar; the Cardiology Department, German Heart Center Munich (A.M., M.B., C.B.J., J.T.L., L.B.-F., T.D., A.G., M.S., D.S., A.S., K.-L.L.); and the Institute of Pharmacology and Toxicology (A.W., F.H.) — all at the Technical University of Munich, Munich, Germany. Address reprint requests to Dr. Laugwitz at the Cardiology Division, First Department of Medicine and German Heart Center Munich, Klinikum rechts der Isar, Technical University of Munich, Ismaninger Str., 22, D-81675 Munich, Germany, or at klaugwitz@med1.med.tum.de.

Drs. Moretti, Bellin, and Welling contributed equally to this article.

This article (10.1056/NEJMoa0908679) was published on July 21, 2010, at NEJM.org.

N Engl J Med 2010;363:1397-1409.

The long-QT syndrome is a familial, usually autosomal dominant disease characterized by an abnormally prolonged ventricular repolarization phase and a propensity toward polymorphic ventricular tachycardia (often termed torsades de pointes) and sudden cardiac death.[1-3] At least 10 different forms of the long-QT syndrome have been described, but in approximately 45% of genotyped patients, the underlying causes are mutations in the *KCNQ1* (also known as *KVLQT1* or *Kv7.1*) gene, which encodes the pore-forming alpha subunits of the channels generating I_{Ks}, an adrenergic-sensitive, slow outward potassium current.[2,4,5] This form of the long-QT syndrome is designated as long-QT syndrome type 1.

Although it is believed that a reduction in I_{Ks} is the cause of the disease phenotype of long-QT syndrome type 1, this has not been established in the case of KCNQ1 channels in human cardiomyocytes. Heterologous expression systems and genetic animal models have been used to determine the underlying mechanisms of the long-QT syndrome; however, cardiac myocytes have distinct and complex electrophysiological properties, and these properties differ among species.[6,7] Thus, a human cell-based system would be extremely useful for understanding the pathogenesis of the disease and for testing patient-specific therapies.[8]

The generation of pluripotent stem cells from human adult somatic tissues[9-13] offers the opportunity to produce large numbers of patient-specific stem cells. In recent studies, investigators have been successful in deriving pluripotent stem cells from individual patients among whom there is a variety of simple and complex genetic disorders and in differentiating them into the specific cell lineages affected by the diseases.[14-19] The capacity of induced human pluripotent stem cells to generate functional cardiac myocytes has been reported,[20-23] but to our knowledge, the use of this approach to generate myocytes harboring a disease phenotype has not yet been shown. In this study, we generated patient-specific pluripotent stem cells from members of a family affected by long-QT syndrome type 1 and showed the capacity of these cells to give rise to functional cardiomyocytes that recapitulate the electrophysiological characteristics of the disorder.

Figure 1 (facing page). Generation of Pluripotent Stem Cells from Patients with Long-QT Syndrome Type 1.

Panel A shows the pedigree of the proband with the long-QT syndrome (Patient III-2; QT interval corrected for heart rate [QTc], 445 msec) and his father (Patient II-2; QTc, 462 msec), as well as his affected aunt and grandfather (QTc, 481 msec and 453 msec, respectively). Squares indicate male family members, circles female family members, solid symbols family members with long-QT syndrome type 1, and open symbols unaffected family members. Panel B shows the results of sequence analysis of genomic KCNQ1 obtained from fibroblasts derived from one of the two control subjects and Patient II-2, revealing a heterozygous missense mutation in KCNQ1 exon 2, in position 569 of the coding sequence (569G→A; NM_000218), resulting in the substitution of the positively charged arginine for an uncharged glutamine at position 190 of the protein (R190Q; NP_000209). The same results were obtained with DNA from all the induced pluripotent stem-cell lines derived from controls and from patients with the long-QT syndrome. Panel C is a schematic representation of the KCNQ1 and KCNE1 proteins, with the R190Q mutation located in the cytoplasmic loop between transmembrane segments S2 and S3 of the KCNQ1 protein. The six transmembrane domains (S1 to S6) are flanked by amino (NH2)–terminal and carboxyl (COOH)–terminal regions; P denotes the pore region. Functional I_{Ks} channels result from the coassembly of four KCNQ1 alpha subunits and at least two auxiliary KCNE1 beta subunits. Panel D shows primary skin fibroblasts derived from Patient II-2 and a representative induced pluripotent stem-cell colony from the same patient. Panel E shows the presence of alkaline phosphatase activity in a representative colony of pluripotent stem cells derived from Patient II-2. Panel F shows immunofluorescence analyses of pluripotency markers NANOG (red) and TRA1-81 (green) in a representative pluripotent stem-cell clone derived from Patient III-2, with nuclear staining (DNA, blue) of all cells, including mouse embryonic fibroblast feeders. The lower right-hand image is a magnification of the area framed in the adjacent image.

METHODS

CLINICAL HISTORY AND GENETIC PHENOTYPE

During the clinical evaluation of an 8-year-old boy for attention deficit–hyperactivity disorder, an electrocardiogram showed a prolonged QT interval (QT interval corrected for heart rate [QTc], 445 msec). Sequencing of the *KCNQ1* gene revealed a heterozygous single base exchange (569G→A), resulting in an R190Q missense mutation previously known to be associated with long-QT syndrome type 1[24-26]

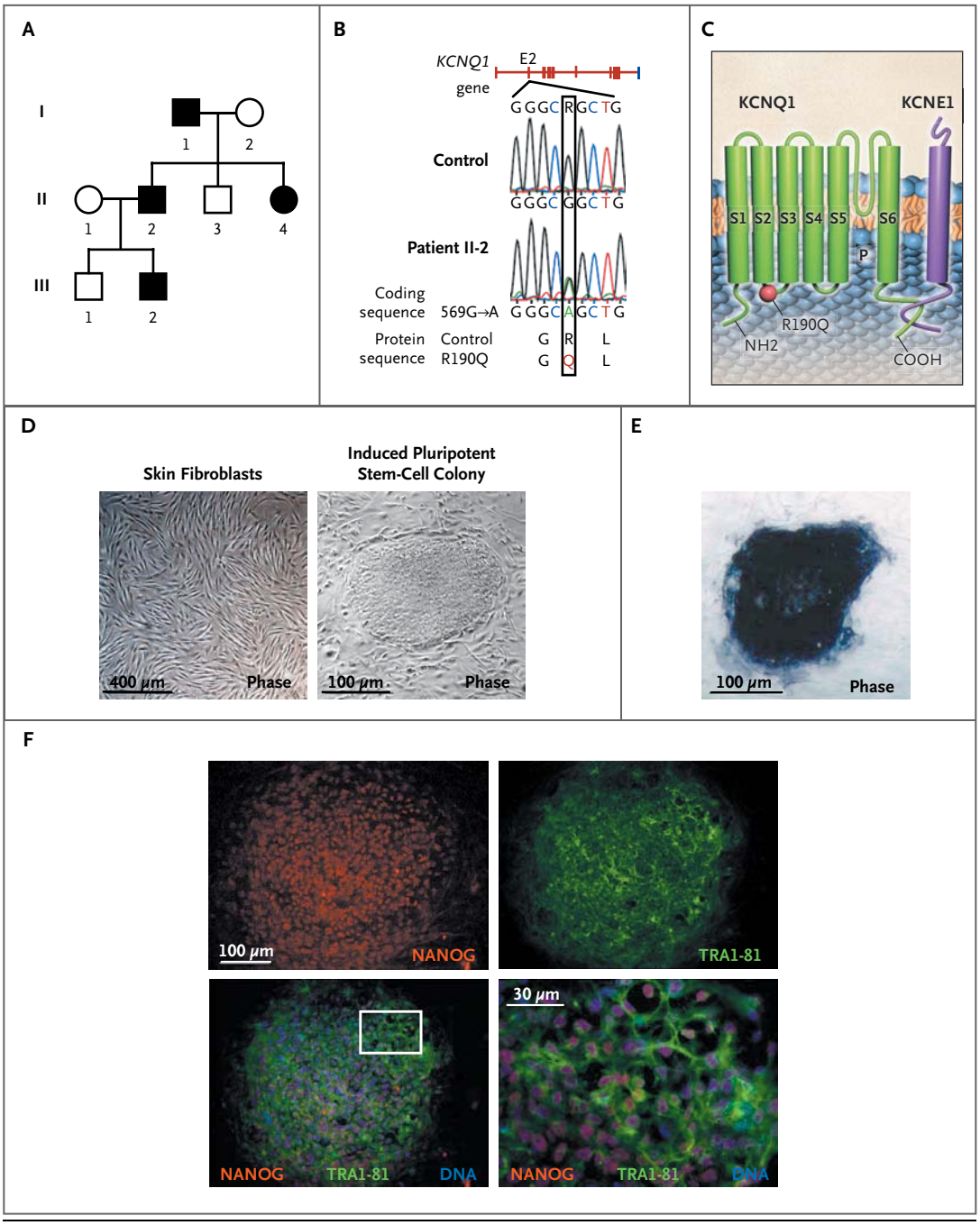

(Fig. 1A and 1B). The mutation is located in the cytoplasmic loop between the transmembrane segments S2 and S3 of the KCNQ1 protein[24] (Fig. 1C).

Subsequent screening of members of the boy's family revealed prolonged QT intervals in the 42-year-old father (QTc, 462 msec), the 39-year-old aunt (QTc, 481 msec), and the 70-year-old grandfather (QTc, 453 msec), and genetic testing showed that these family members had the same heterozygous mutation, confirming autosomal dominant inheritance in this family (Fig. 1A and 1B). The father and son have thus far been as-

ymptomatic. The grandfather and aunt have reported periods of dizziness and palpitations. All the genetically affected family members are being treated with beta-blockers.

GENERATION OF PATIENT-SPECIFIC PLURIPOTENT STEM CELLS

For the generation of pluripotent stem cells, we recruited the father and son in the family affected by long-QT syndrome type 1 along with two healthy control subjects. The protocols for research involving human subjects and for stem-cell research were approved by the institutional review board and the committee charged with oversight of embryonic stem-cell research at the Technical University of Munich. All the study participants provided written informed consent.

Dermal-biopsy specimens were minced and placed on culture dishes. Fibroblasts migrating out of the explants were passaged twice and then infected with a combination of retroviruses encoding the human transcription factors OCT3/4, SOX2, KLF4, and c-MYC.[9] After 6 days, infected cells were seeded on murine embryonic fibroblast feeders and cultured in standard human embryonic stem-cell medium until induced pluripotent stem-cell colonies appeared. Details of the study methods are provided in the Supplementary Appendix, available with the full text of this article at NEJM.org.

IN VITRO CARDIAC DIFFERENTIATION

We differentiated induced pluripotent stem cells as embryoid bodies by detaching the stem-cell colonies from the feeder cells and maintaining them for 3 days in feeder-cell-conditioned human embryonic stem-cell medium in low attachment plates.[27,28] At day 4, the medium was replaced with differentiation medium containing 20% fetal-calf serum. Embryoid bodies were plated on gelatin-coated dishes on day 7. Between days 20 and 30, areas that exhibited spontaneous contraction (indicative of cardiac differentiation) were microdissected, plated on fibronectin-coated plates, and maintained in culture in differentiation medium containing 2% fetal-calf serum. For single-cell analysis, microdissected areas were dissociated with the use of type II collagenase. Single cells were plated on fibronectin-coated slides for immunohistochemical and electrophysiological analysis.

IMMUNOHISTOCHEMICAL ASSESSMENTS

Immunostaining was performed according to standard protocols with the use of antibodies specific for the following: Nanog (Abcam), TRA-1-81 (BD Pharmingen), cardiac troponin T (Lab Vision), α-actinin (Sigma–Aldrich), myosin light chain 2a and myosin light chain 2v (Synaptic Systems), KCNQ1 (Abcam), and protein disulfide isomerase (Abcam). Staining was also performed for F-actin with the use of fluorescence-labeled phalloidin (Invitrogen).

POLYMERASE-CHAIN-REACTION ASSAYS

The polymerase chain reaction (PCR) was used to amplify the mutated region of the *KCNQ1* gene for sequencing. Quantitative real-time PCR was used in allelic-discrimination assays and for the assessment of expression of pluripotency genes, retroviral transgenes, and cell-lineage markers. Reverse-transcriptase (RT)–PCR was used to assay cardiomyocyte phenotype markers in single cells. Detailed methods are provided in the Supplementary Appendix; primers are listed in Table 1 in the Supplementary Appendix.

ELECTROPHYSIOLOGICAL ASSESSMENTS

Whole-cell recordings were obtained with the use of standard patch-clamp techniques.[7,29] Culture differentiation medium was used as the external bath solution. Action potentials and currents were recorded at approximately 35°C. All currents were normalized to cell capacitance.

STATISTICAL ANALYSIS

Data that passed tests for normality and equal variance were analyzed with the use of one-way analysis of variance followed by Tukey's test, when appropriate. The Wilcoxon signed-rank test and the Kruskal–Wallis test followed by Dunn's test were used to analyze the remaining data. Two-sided P values of less than 0.05 were considered to indicate statistical significance.

RESULTS

GENERATION OF PLURIPOTENT STEM CELLS

We generated pluripotent stem cells from primary fibroblasts derived from two patients with long-QT syndrome type 1 and two control subjects after retroviral transduction of the reprogramming factors. Starting at 3 weeks after viral

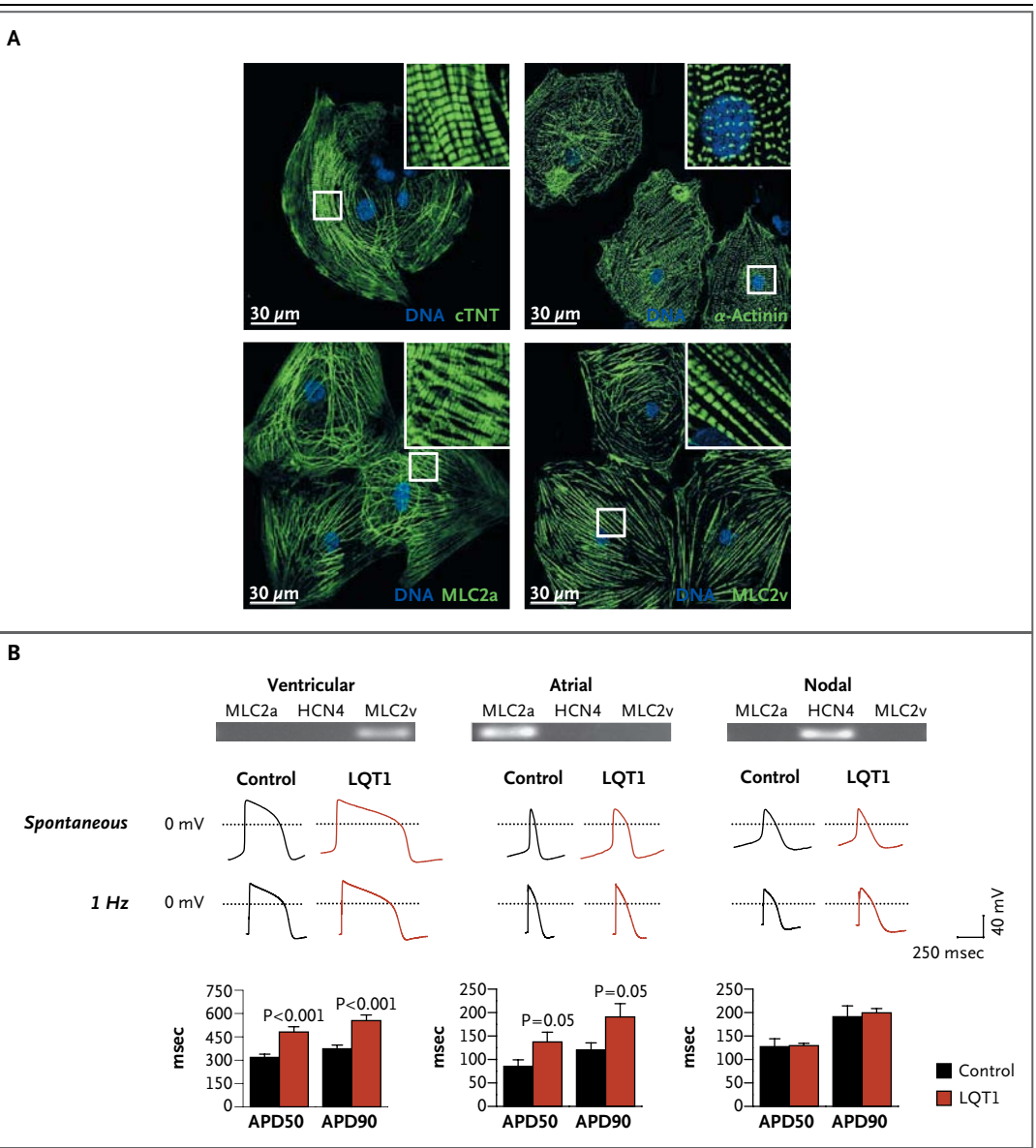

Figure 2. Disease Phenotype of Long-QT Syndrome Type 1 Cardiac Myocytes Generated from Induced Pluripotent Stem Cells.

Panel A shows immunofluorescence analysis for cardiomyocyte markers in single cells dissociated from long-QT syndrome type 1 (LQT1) explants. The insets, which are magnifications of the framed areas, show the organization of cardiac troponin T (cTNT), α-actinin, and atrial and ventricular isoforms of myosin light chain 2 (MLC2a and MLC2v) into mature sarcomeric structures. The top of Panel B shows the results of single-cell RT-PCR from three representative patched cells with respect to the expression of specific myocyte markers: MLC2v, MLC2a, and hyperpolarization-activated, cyclic nucleotide-gated channel 4 (HCN4). The middle of the panel shows examples of typical spontaneous and paced (at 1 Hz) "ventricular," "atrial," and "nodal" action potentials recorded in cardiomyocytes derived from induced pluripotent stem cells from a control subject and a patient with LQT1. The bar graphs at the bottom of the panel represent the averaged action-potential duration at 50% repolarization (APD50) and at 90% repolarization (APD90) for each of the three myocyte subtypes at a 1-Hz stimulation rate. Between 4 and 40 cells from six different induced pluripotent stem-cell clones (three clones from each person) were analyzed per group (see Table 3 in the Supplementary Appendix). P values are for the comparison between LQT1 myocytes and control myocytes, with the use of one-way analysis of variance.

infection, colonies with stem-cell morphologic characteristics appeared and were clonally expanded on murine embryonic fibroblasts (Fig. 1D). Three clones from each subject were chosen for further characterization.

The genomic *KCNQ1* locus was sequenced in all the induced pluripotent stem-cell clones, confirming the integrity of the locus and the absence of retroviral DNA. The expected 569G→A mutation was detected in all stem-cell clones and skin fibroblasts derived from the patients with long-QT syndrome type 1 but not in cells derived from control subjects. The presence of alkaline phosphatase activity (Fig. 1E), immunoreactivity for embryonic stem-cell–associated antigens, including NANOG and TRA-1-81 (Fig. 1F), reactivation of endogenous pluripotency genes (*OCT3/4, SOX2, REX1, NANOG,* and *CRIPTO/TDGF1*) (Fig. 1A in the Supplementary Appendix), and silencing of retroviral transgenes (Fig. 1B in the Supplementary Appendix) indicated that there had been successful reprogramming of putative induced pluripotent stem-cell clones. On spontaneous embryoid-body differentiation, all induced pluripotent stem-cell clones showed up-regulation of lineage markers representative of the three embryonic germ layers, endoderm (*PDX1*, *SOX7*, and *AFP*), mesoderm (*CD31*, *DESMIN*, *ACTA2*, *SCL*, *MYL2*, and *CDH5*), and ectoderm (*KTR14*, *NCAM1*, *TH*, and *GABRR2*) (Fig. 2 in the Supplementary Appendix), confirming their pluripotent nature.[28]

ASSESSMENT OF THE LONG-QT SYNDROME TYPE 1 PHENOTYPE

Using a specific differentiation protocol, we directed induced pluripotent stem cells from both affected family members and controls into the cardiac lineage (see Methods, Results, and Fig. 3 in the Supplementary Appendix). Spontaneously contracting foci started to appear after approximately 12 days of differentiation (see video 1, available at NEJM.org) and were explanted and then dissociated into single cells that maintained the expression of distinct myocyte markers (Fig. 2A) and spontaneous contraction (video 2). No major differences in the efficiency of differentiation into myocyte lineages were observed among the three clones from each of the four subjects (Fig. 3E in the Supplementary Appendix).

To assess whether the myocytes derived from induced pluripotent stem cells from patients with long-QT syndrome type 1 recapitulated the disease phenotype, we recorded the action potentials in single cells. Both spontaneously beating cells that had been dissociated from long-QT syndrome type 1 explants and those that had been dissociated from control explants responded to pacing and generated three distinct types of action potentials. These were designated as "ventricular," "atrial," and "nodal," on the basis of their similarity to the action potentials of ventricular, atrial, and nodal cardiomyocytes from human fetal hearts[30] (Fig. 2B; for detailed classification, see Results, Discussion, and Fig. 4 in the Supplementary Appendix). The classification based on action-potential properties correlated with gene-expression analysis of specific myocyte-lineage markers, as shown with the use of single-cell RT-PCR on patched cells (Fig. 2B, and Fig. 4 and 5 in the Supplementary Appendix).

Whereas the characteristics of the action potential of "nodal" myocytes were similar between cells derived from patients with long-QT syndrome type 1 and cells derived from control subjects, the action potentials of "ventricular" and "atrial" myocytes derived from patients with long-QT syndrome type 1 were significantly longer and had a slower repolarization velocity than did those derived from controls (Fig. 2B, and Tables 2 and 3 in the Supplementary Appendix). With electrical pacing set at 1 Hz, the mean (±SE) duration of the action potential measured at 90% repolarization was 554.2±35.6 msec and 190.8±28.1 msec in "ventricular" and "atrial" myocytes, respectively, in cells derived from patients with long-QT syndrome type 1, as compared with 373.2±22.6 msec and 119.9±15.5 msec in the corresponding cells from control subjects (Fig. 2B). Increasing the stimulation frequency decreased the duration of the "ventricular" myocyte action potential in both groups, with little change in other features of the action potential. However, adaptation of the action-potential duration to higher pacing frequencies was significantly less pronounced in the myocytes from the patients with long-QT syndrome type 1 than in those from the control subjects (Fig. 6 in the Supplementary Appendix). The results were similar in all the clones from the two patients and in all the clones from the two healthy controls (Fig. 7 in the Supplementary Appendix), suggesting that there was phenotypic homogeneity among

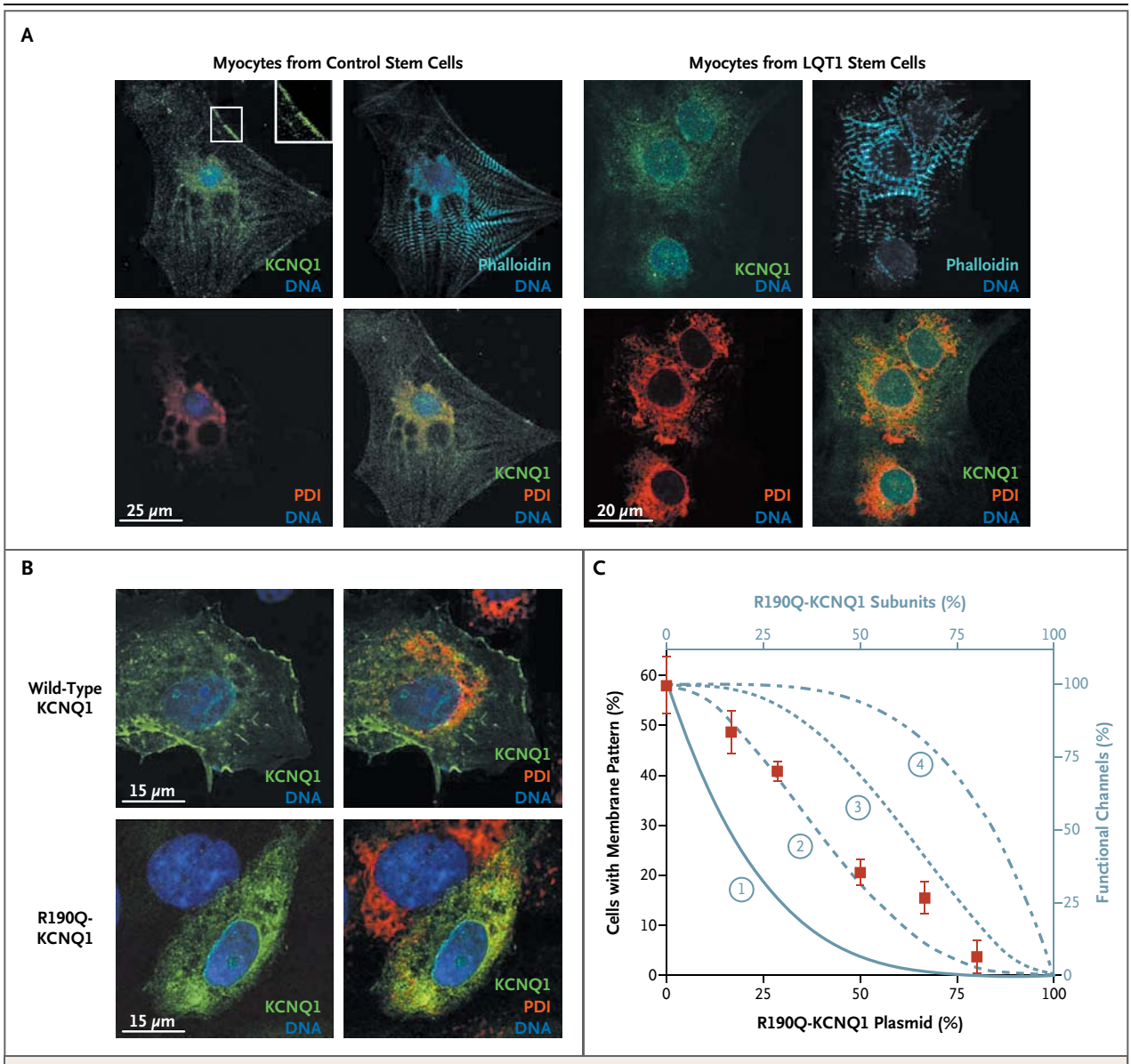

Figure 3. Characterization of the Role of the R190Q-KCNQ1 Mutation in the Pathogenesis of Long-QT Syndrome Type 1.

Panel A shows immunofluorescence analysis of the cellular distribution of KCNQ1 in representative myocytes derived from induced pluripotent stem cells from a control subject and a patient with long-QT syndrome type 1. KCNQ1 (green) can be seen in the endoplasmic reticulum, stained by protein disulfide isomerase (PDI, red), and on the plasma membrane (inset in upper left-hand image) of control myocytes but remains mostly in the endoplasmic reticulum of long-QT syndrome type 1 myocytes. Phalloidin staining (cyan) was used to identify differentiated striated myocytes. Panel B shows immunofluorescence analysis of the cellular distribution of KCNQ1 in H9c2 cells transfected with wild-type or R190Q-KCNQ1 expression vector. Wild-type KCNQ1 (green, upper images) is enriched in the plasma membrane of the cell, whereas R190Q-KCNQ1 (green, lower images) shows aberrant membrane translocation. Panel C shows the effect of cotransfecting increasing amounts of an expression vector encoding R190Q-KCNQ1, fused to a cyan fluorescent protein, together with a constant amount of a construct expressing wild-type KCNQ1, fused to yellow fluorescent protein, on the percentage of cells displaying yellow fluorescence in a plasma membrane or vesicular staining pattern (experimental data shown in red, with I bars indicating standard errors). The expected percentage of functional channels is plotted against the percentage of available R190Q-KCNQ1 subunits, assuming that the presence of 1, 2, 3, or 4 R190Q-KCNQ1 subunits (indicated by the encircled numbers) in a channel tetramer is sufficient to render the channel nonfunctional.

induced pluripotent stem-cell lines from the same person and no evident difference in the disease phenotype of the cells from the two patients with long-QT syndrome type 1. Therefore, we limited our further analysis to three clones from one patient with long-QT syndrome type 1 and three clones from one control subject.

ROLE OF R190Q-KCNQ1 IN THE PATHOGENESIS OF LONG-QT SYNDROME TYPE 1

The analysis of gene expression with the use of quantitative RT-PCR and immunoblotting revealed that *KCNQ1* messenger RNA and protein levels were similar between myocytes derived from subjects with long-QT syndrome type 1 and those derived from controls. In addition, there was similar allelic expression of wild-type and mutated 569G→A transcripts in explants derived from two different clones from the patient with long-QT syndrome type 1 (Fig. 8 in the Supplementary Appendix). To further investigate the functional consequences of the R190Q-KCNQ1 mutation in the induced pluripotent stem-cell model, we examined the cellular distribution of the KCNQ1 protein. Immunocytochemical tests for KCNQ1 in myocytes derived from patients with long-QT syndrome type 1 revealed a reticular, intracellular expression pattern, in which KCNQ1 partially colocalized with the endoplasmic-reticulum marker protein disulfide isomerase. In contrast, in cells from control subjects, the channel subunit was enriched in the cell surface compartment (Fig. 3A). Arginine 190 of KCNQ1 is known to be part of a basic endoplasmic-reticulum retention signal.[31,32] This suggests that the subcellular distribution of KCNQ1 observed in myocytes derived from patients with long-QT syndrome type 1 may be due to a trafficking defect.

To confirm this hypothesis, we expressed R190Q-KCNQ1 subunits and wild-type KCNQ1 subunits in the cardiomyoblast H9c2 cell line and analyzed their subcellular localization. As was seen in the immunodetection pattern of KCNQ1 in induced pluripotent stem-cell–derived myocytes, wild-type KCNQ1 protein achieved cell-membrane targeting, whereas R190Q-KCNQ1 failed to do so (Fig. 3B). Expression vectors encoding wild-type KCNQ1, fused to a yellow fluorescent protein, and R190Q-KCNQ1, fused to a cyan fluorescent protein, were then cotransfected into H9c2 cells in various ratios. The percentage of cells presenting a yellow fluorescent protein signal in a cell membrane pattern decreased as the proportion of mutant channel subunits increased, suggesting a model in which a tetrameric channel containing more than one R190Q subunit loses the ability to translocate to the cell

Figure 4 (facing page). Electrophysiological Analysis of I_K Current in Myocytes Derived from Induced Pluripotent Stem Cells from Control Subjects and from Patients with Long-QT Syndrome Type 1.

Panel A shows the isolation of the slow and rapid components of I_K (I_{Ks} and I_{Kr}) in "ventricular" myocytes from induced pluripotent stem cells. The graphs on the left show sample traces of whole-cell current from control and long-QT syndrome type 1 (LQT1) cells and the voltage protocol used for the recordings. The holding potential was at −40 mV, and test potentials were at +10, +30, and +50 mV, lasting 5 seconds. Tail current was recorded after the test potential was back to −40 mV. After a recording without drugs (a and a′), the cells were perfused with 10 μM chromanol 293B (b) or with 1 μM E4031 (b′), and I_{Ks} and I_{Kr} were defined as the chromanol-sensitive (c) and E4031-sensitive (c′) currents, respectively. The graphs on the right show quantification of I_{Ks} and I_{Kr}. Current amplitudes measured at the end of depolarization (I_{Ks} or I_{Kr}) and at the peak of the tail (I_{Ks} tail or I_{Kr} tail) were plotted against membrane voltages. The control myocytes included 9 cells from three induced pluripotent stem-cell clones derived from one of the control subjects, and the LQT1 myocytes included 12 cells from three clones derived from Patient II-2. There was a significant reduction in I_{Ks} current density in LQT1 cells as compared with control cells at the specified membrane voltages. Asterisks denote $P<0.05$, with the use of one-way analysis of variance. Current density is measured as picoamperes per picofarad (pA/pF). Panel B shows the voltage dependence of I_{Ks} activation. Peak values of chromanol-sensitive I_{Ks} tail currents were normalized to the maximum amplitude value recorded from each particular cell and plotted against the test potentials. The holding potential was at −40 mV, and test potentials were at 0 to +50 mV, in steps of 10 mV, each lasting 5 seconds. The control "ventricular" myocytes included 7 cells from three clones derived from one of the control subjects, and LQT1 "ventricular" myocytes included 8 cells from three clones derived from Patient II-2. Panel C shows the voltage dependence of I_{Ks} deactivation kinetics. I_{Ks} was activated by a 5-second test pulse to +50 mV from a holding potential of −40 mV. The cells were then clamped back to different potentials ranging from −40 to −10 mV, and the deactivation time course of the tail current was fitted by a single exponential function. Measurements were performed in the presence of 1 μM E4031 in order to block I_{Kr}. The graph shows the time constant (τ) of deactivation plotted against the membrane potential. The control "ventricular" myocytes included 7 cells from two clones derived from one of the control subjects, and LQT1 "ventricular" myocytes included 8 cells from two clones derived from Patient II-2. $P<0.05$, with the use of a one-way analysis of variance.

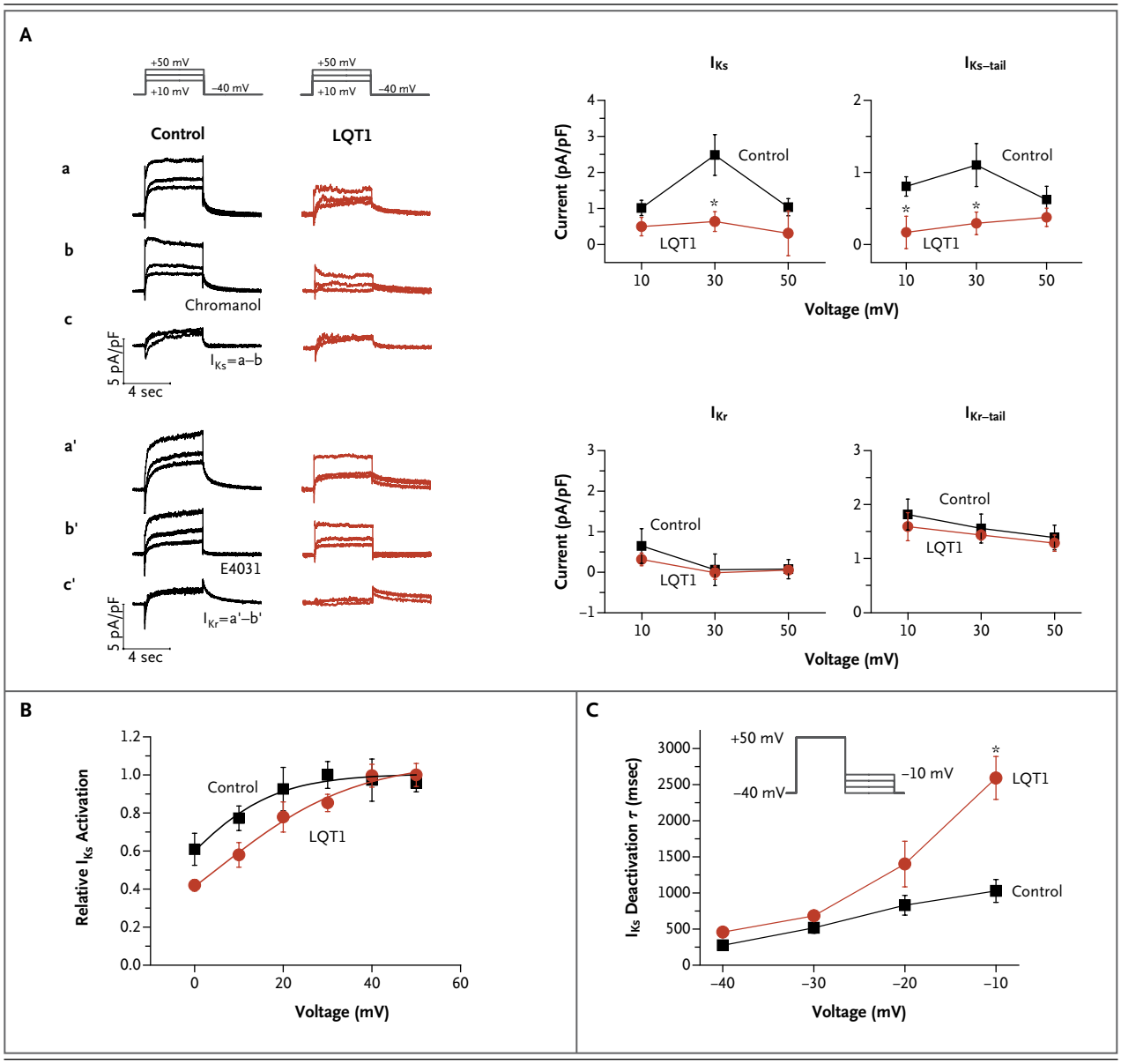

surface compartment (Fig. 3C; for details on the model, see the Methods section in the Supplementary Appendix). Analysis of fluorescence resonance energy transfer showed that the R190Q mutation did not alter the capacity of the mutant subunit to coassemble with wild-type subunits (Fig. 9 in the Supplementary Appendix).[33]

ELECTROPHYSIOLOGICAL ANALYSIS OF K+ CURRENTS

To provide further mechanistic insight into the function of the mutated KCNQ1 protein, we performed single-cell electrophysiological analysis of various repolarizing K^+ currents in "ventricular" myocytes. With the use of a distinct voltage protocol that preferentially elicits the outward delayed rectifier current, I_K, cardiac myocytes derived from induced pluripotent stem cells from patients with long-QT syndrome type 1, as compared with those from control subjects, showed a substantial reduction in K^+ current (Fig. 4A).

Further characterization with the use of channel blockers specific for the slow and rapid components of I_K — chromanol 293B (which blocks I_{Ks}) and E4031 (which blocks I_{Kr})[34] — showed that I_{Ks} current densities in myocytes from patients with long-QT syndrome type 1, as compared with those from control subjects, were decreased, whereas I_{Kr} conductance was unaffected. At +30

mV, I_{Ks} and tail I_{Ks} were diminished by approximately 75%, suggesting that in heterozygous "ventricular" myocytes from patients with long-QT syndrome type 1, the mutant form of KCNQ1 interferes with the function of the wild-type subunit (Fig. 4A). Furthermore, both activation and deactivation properties of the tail I_{Ks} current in cells from patients with long-QT syndrome type 1, as compared with cells from controls, appeared to be altered, with activation being slightly shifted toward more positive voltages (Fig. 4B) and deactivation being decelerated (Fig. 4C). We next analyzed the transient outward (I_{to}) and inward currents that function in the hyperpolarization state. As with the results for I_{Kr}, I_{to} and diastolic current densities did not differ between "ventricular" myocytes from patients with long-QT syndrome type 1 and those from control subjects (Fig. 10 in the Supplementary Appendix), showing that there was a specific genotype–phenotype correlation.

PROTECTIVE ACTION OF BETA-BLOCKADE

Since fatal arrhythmias are precipitated by increased sympathetic tone in patients with long-QT syndrome type 1,[3,35] we tested whether adrenergic stimulation can affect the phenotype of long-QT syndrome type 1 cardiomyocytes derived from pluripotent stem cells. First, we analyzed the effect of catecholamines on the duration of the action potential in paced "ventricular" myocytes. At 2 Hz, isoproterenol induced approximately a 20% reduction in the interval between 30% and 90% repolarization of the action potential in control myocytes, whereas in cells from patients with long-QT syndrome type 1 this interval was almost unaffected (Fig. 5A). Accordingly, I_{Ks} was markedly enhanced by adrenergic stimulation in "ventricular" myocytes from control subjects, and the increase was significantly smaller in cells from patients with long-QT syndrome type 1, suggesting that defective responsiveness to adrenergic challenge is due to an abnormal I_{Ks} current (Fig. 5B).[36]

We further investigated the effect of isoproterenol on spontaneously beating myocytes. In cells from control subjects, isoproterenol had a positive chronotropic effect accompanied by a shortening of the duration of the action potential, resulting in a 30% reduction in the ratio of the action-potential duration at 90% repolarization to the action-potential interval. In contrast, in myocytes from patients with long-QT syndrome type 1, this ratio was increased by 15%, thereby exacerbating the long-QT syndrome type 1 phenotype and increasing the risk of arrhythmic events (Fig. 5C). In fact, under conditions of adrenergic stress, six of nine "ventricular" myocytes from patients with long-QT syndrome type 1 developed early afterdepolarizations (4.1±1.5 early

Figure 5 (facing page). Adrenergic Modulation and Protective Effect of Beta-Blockade in Control and Long-QT Syndrome Type 1 "Ventricular" Myocytes.

Panel A shows an overlay of single action potentials from a representative cell from a control subject and from a patient with long-QT syndrome type 1 (LQT1) at a 2-Hz stimulation rate before (basal) and after application of 100 nM isoproterenol. The bar graph represents the percent change induced by isoproterenol on the interval from the action-potential duration (APD) at 30% repolarization (APD30) to APD90 (APD30–APD90), on APD90, and on APD. Data are means ±SE for 10 cells in each group (from three clones derived from one of the control subjects and three clones derived from Patient II-2). Panel B shows the effect of adrenaline on I_{Ks} tail current. On the left are representative overlapped I_{Ks} tail-current traces from a control and an LQT1 myocyte before and after treatment with 1 μM adrenaline recorded at +30 mV depolarization with the use of the voltage protocol depicted at the top of the panel. Measurements were performed in presence of 1 μM E4031 in order to block I_{Kr}. The bar graph represents the factor increase in I_{Ks} tail current induced by 1 μM adrenaline at the specified depolarization voltages in control and LQT1 myocytes. Data are means ±SE for 8 cells in each group (from two clones derived from one of the control subjects and from two clones derived from Patient II-2). Panel C shows representative recordings of single-cell spontaneous action potentials from a control and an LQT1 "ventricular" myocyte before (baseline) and during exposure to a combination of 100 nM isoproterenol and 200 nM propranolol or to 100 nM isoproterenol alone. Cells were pretreated for 2 minutes with 200 nM propranolol before application of the combination of 100 nM isoproterenol and 200 nM propranolol (traces not shown). The bar graph represents the percent change in the ratio of APD90 to the action-potential interval (APD90/AP interval) induced by the combination of 100 nM isoproterenol and 200 nM propranolol or by 100 nM isoproterenol alone. Action potentials affected by early afterdepolarizations (EAD) were excluded from the analysis. Data are means ±SE for 8 control cells (from three clones derived from one of the control subjects) and 9 LQT1 cells (from three clones derived from Patient II-2). P values in the three panels are for the comparison between LQT1 myocytes and control myocytes, with the use of the Wilcoxon signed-rank test.

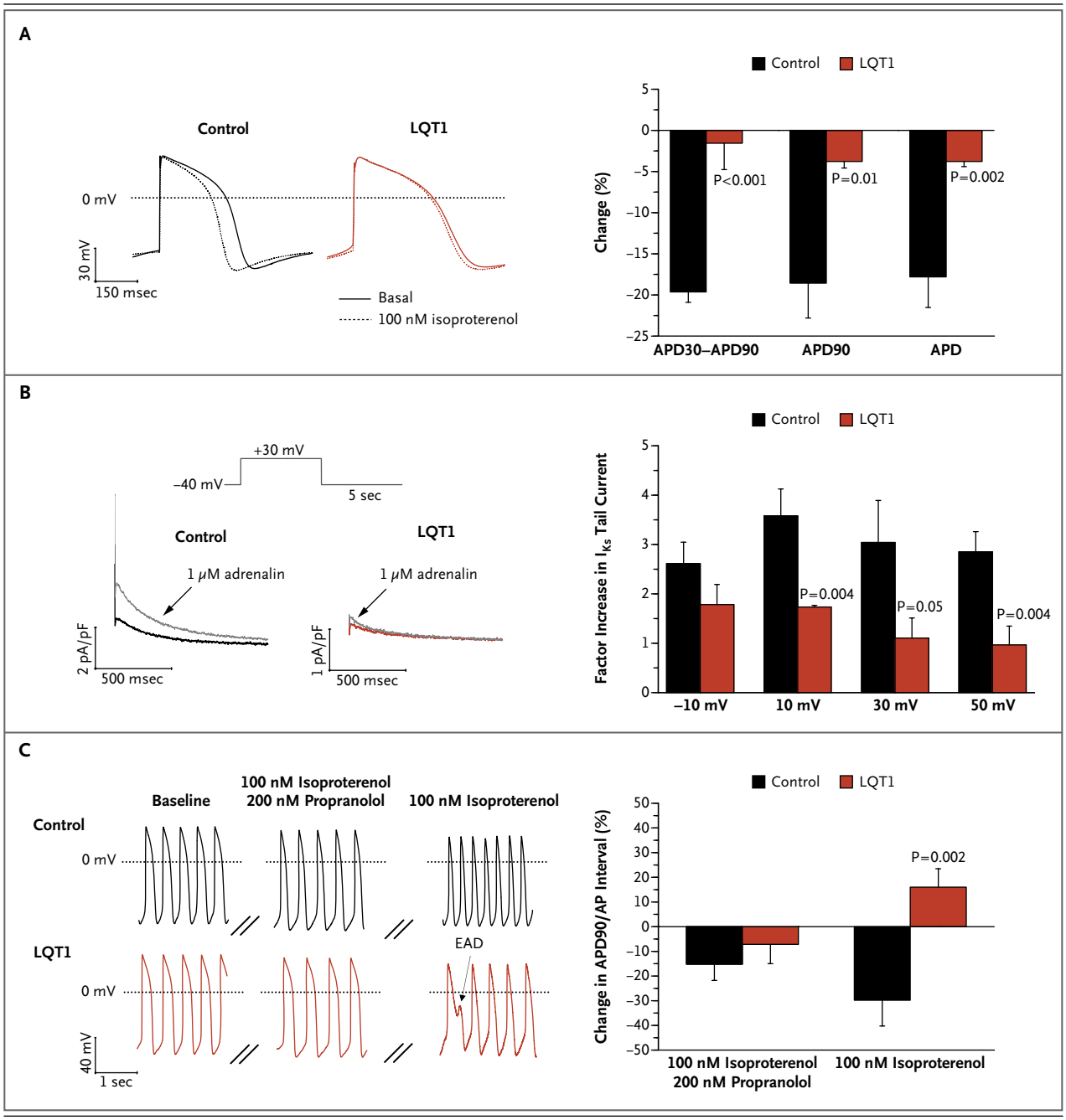

afterdepolarizations per 20 sec, with 9.2±2.1% of the beats affected by early afterdepolarizations), whereas none of the eight cells from control subjects did. Pretreatment with propranolol, a nonselective beta-blocker, substantially blunted the effect of isoproterenol in myocytes from both control subjects and patients with long-QT syndrome type 1 (0.6±0.3 early afterdepolarizations per 20 sec, with 1.7±0.8% of the beats affected), thus protecting the diseased cells from catecholamine-induced tachyarrhythmia due to impaired rate adaptation of the action potential (Fig. 5C).

DISCUSSION

Since the initial reports on induced human pluripotent stem-cell technology were published, several patient-specific induced pluripotent stem-

cell lines for neurodegenerative and metabolic disorders have been developed.[14,16,18,19,37] Establishing reliable models of human disease in such cells has remained challenging, owing to difficulties in directing cell differentiation and in identifying disease-related mechanisms. In this study, we reprogrammed fibroblasts derived from members of a family with autosomal-dominant long-QT syndrome type 1 and used these induced pluripotent stem cells to generate patient-specific cardiomyocytes. These myocytes showed expression of specific markers and electrophysiological characteristics that suggested that the reprogramming process did not affect the ability of the cells to function normally. Furthermore, we observed disease-specific abnormalities in the duration of the action potential, the action-potential rate adaptation, and I_{Ks} currents, owing to an R190Q-KCNQ1 trafficking defect, as well as vulnerability to catecholaminergic stress.

To date, insights into the pathogenesis of the long-QT syndrome have come primarily from heterologous expression systems and genetic animal models. Depending on the cell type used, both haploinsufficiency and dominant negative effects have been postulated as the mechanism of disease associated with the R190Q mutation.[24-26] In our induced pluripotent stem-cell model of long-QT syndrome type 1, a reduction in I_{Ks} current density by approximately 75%, combined with subcellular localization, showed that the R190Q mutant suppresses channel trafficking to the plasma membrane in a dominant negative manner. Owing to differences among species in the channels that generate the main cardiac repolarizing currents, none of the available mouse models of the long-QT syndrome fully emulate the human disease phenotype. Recently, transgenic rabbit models of long-QT syndrome type 1 and long-QT syndrome type 2 have been engineered by means of overexpression of dominant negative pore mutants of the human genes *KCNQ1* and *KCNH2*.[38] In these animals, both transgenes caused a down-regulation of the complementary I_{Kr} and I_{Ks} currents. In contrast, no alterations in repolarizing currents other than in I_{Ks} were observed in patient-specific myocytes derived from persons with the R190Q-KCNQ1 mutation associated with long-QT syndrome type 1. This discrepancy, which may be mutant-dependent or model-dependent, shows the importance of alternative systems in which human genetic disorders can be studied in the physiologic and disease-causing contexts on a patient-specific level.

Our data provide clear evidence that the pathogenesis of the R190Q mutation can be modeled in myocyte lineages generated from pluripotent stem cells derived from patients with long-QT syndrome type 1. Moreover, our findings suggest that there may be alternative approaches to the development of candidate drugs, such as compounds to promote the delivery of the mutant to the plasma membrane or I_{Ks} activators. The observed protective effects of beta-blockade show that it is possible to investigate the therapeutic action of medications for treating human cardiac disease in vitro with the use of patient-specific cells. This approach is particularly attractive because of the pluripotent nature of these cells and the potentially unlimited number of induced cardiomyocytes available for high-throughput drug development.

Even though the incidence of the long-QT syndrome is only 1 case per 2500 live births, this syndrome provides a platform for showing the suitability of induced pluripotent stem-cell technology as a means of exploring disease mechanisms in human genetic cardiac disorders. Larger sets of long-QT syndrome cell lines harboring different channel mutations will be needed to further validate the disease phenotype and compare pathogenetic mechanisms in diverse forms of the disease. Clinically, the severity of manifestations of the long-QT syndrome varies among family members, and incomplete penetrance exists.[39] However, we did not observe any phenotypic differences in the prolongation of the action potential between the myocytes from our two patients, a finding that is probably due to the similarity of the clinical phenotype in these cases.

In summary, we derived pluripotent stem cells from patients with long-QT syndrome type 1 and directed them to differentiate into cardiac myocytes. As compared with myocytes derived in a similar fashion from healthy controls, cells from patients with long-QT syndrome type 1 exhibited prolongation of the action potential, altered I_{Ks} activation and deactivation properties, and an abnormal response to catecholamine stimulation, with a protective effect of beta-blockade, thus showing that induced pluripotent stem-cell models can recapitulate aspects of genetic cardiac diseases.

Supported by grants from the European Research Council (Marie Curie Excellence Team Grant, MEXT-23208), the German Research Foundation (Research Unit 923 and La 1238 3-1/4-1), and the German Ministry for Education and Research (01 GN 0826).

Disclosure forms provided by the authors are available with the full text of this article at NEJM.org

We thank Takashi Kitamura and Shinya Yamanaka for providing viral vectors through Addgene; Jacques Barhanin for KCNE1 and wild-type and mutant (R190Q) KCNQ1 complementary DNAs; Stefan Engelhardt and Andrea Ahles for the fluorescent β1-receptor fusion construct; Diana Grewe, Christina Scherb, and Sabine Teuber for their technical assistance in cell culture and immunohistochemical assessments; and especially the members of the family affected by long-QT syndrome type 1 and the healthy volunteers who provided us with skin-biopsy specimens for the reprogramming.

REFERENCES

1. Priori SG, Bloise R, Crotti L. The long QT syndrome. Europace 2001;3:16-27.
2. Moss AJ, Shimizu W, Wilde AA, et al. Clinical aspects of type-1 long-QT syndrome by location, coding type, and biophysical function of mutations involving the KCNQ1 gene. Circulation 2007;115:2481-9.
3. Roden DM. Long-QT syndrome. N Engl J Med 2008;358:169-76.
4. Li GR, Feng J, Yue L, Carrier M, Nattel S. Evidence for two components of delayed rectifier K+ current in human ventricular myocytes. Circ Res 1996;78:689-96.
5. Marx SO, Kurokawa J, Reiken S, et al. Requirement of a macromolecular signaling complex for beta adrenergic receptor modulation of the KCNQ1-KCNE1 potassium channel. Science 2002;295:496-9.
6. Hofmann F, Lacinová L, Klugbauer N. Voltage-dependent calcium channels: from structure to function. Rev Physiol Biochem Pharmacol 1999;139:33-87.
7. Ludwig A, Zong X, Jeglitsch M, Hofmann F, Biel M. A family of hyperpolarization-activated mammalian cation channels. Nature 1998;393:587-91.
8. Laugwitz KL, Moretti A, Caron L, Nakano A, Chien KR. Islet1 cardiovascular progenitors: a single source for heart lineages? Development 2008;135:193-205.
9. Takahashi K, Tanabe K, Ohnuki M, et al. Induction of pluripotent stem cells from adult human fibroblasts by defined factors. Cell 2007;131:861-72.
10. Yu J, Vodyanik MA, Smuga-Otto K, et al. Induced pluripotent stem cell lines derived from human somatic cells. Science 2007;318:1917-20.
11. Park IH, Zhao R, West JA, et al. Reprogramming of human somatic cells to pluripotency with defined factors. Nature 2008;451:141-6.
12. Lowry WE, Richter L, Yachechko R, et al. Generation of human induced pluripotent stem cells from dermal fibroblasts. Proc Natl Acad Sci U S A 2008;105:2883-8.
13. Jaenisch R, Young R. Stem cells, the molecular circuitry of pluripotency and nuclear reprogramming. Cell 2008;132:567-82.
14. Dimos JT, Rodolfa KT, Niakan KK, et al. Induced pluripotent stem cells generated from patients with ALS can be differentiated into motor neurons. Science 2008;321:1218-21.
15. Park IH, Arora N, Huo H, et al. Disease-specific induced pluripotent stem cells. Cell 2008;134:877-86.
16. Ebert AD, Yu J, Rose FF Jr, et al. Induced pluripotent stem cells from a spinal muscular atrophy patient. Nature 2009;457:277-80.
17. Raya A, Rodríguez-Pizà I, Guenechea G, et al. Disease-corrected haematopoietic progenitors from Fanconi anaemia induced pluripotent stem cells. Nature 2009;460:53-9.
18. Soldner F, Hockemeyer D, Beard C, et al. Parkinson's disease patient-derived induced pluripotent stem cells free of viral reprogramming factors. Cell 2009;136:964-77.
19. Maehr R, Chen S, Snitow M, et al. Generation of pluripotent stem cells from patients with type 1 diabetes. Proc Natl Acad Sci U S A 2009;106:15768-73.
20. Zhang J, Wilson GF, Soerens AG, et al. Functional cardiomyocytes derived from human induced pluripotent stem cells. Circ Res 2009;104(4):e30-e41.
21. Yokoo N, Baba S, Kaichi S, et al. The effects of cardioactive drugs on cardiomyocytes derived from human induced pluripotent stem cells. Biochem Biophys Res Commun 2009;387:482-8.
22. Gai H, Leung EL, Costantino PD, et al. Generation and characterization of functional cardiomyocytes using induced pluripotent stem cells derived from human fibroblasts. Cell Biol Int 2009;33:1184-93.
23. Freund C, Davis RP, Gkatzis K, Ward-van Oostwaard D, Mummery CL. The first reported generation of human induced pluripotent stem cells (iPS cells) and iPS cell-derived cardiomyocytes in the Netherlands. Neth Heart J 2010;18:51-4.
24. Chouabe C, Neyroud N, Richard P, et al. Novel mutations in KvLQT1 that affect Iks activation through interactions with Isk. Cardiovasc Res 2000;45:971-80.
25. Donger C, Denjoy I, Berthet M, et al. KVLQT1 C-terminal missense mutation causes a forme fruste long-QT syndrome. Circulation 1997;96:2778-81.
26. Wang Z, Tristani-Firouzi M, Xu Q, Lin M, Keating MT, Sanguinetti MC. Functional effects of mutations in KvLQT1 that cause long QT syndrome. J Cardiovasc Electrophysiol 1999;10:817-26.
27. Moretti A, Caron L, Nakano A, et al. Multipotent embryonic isl1+ progenitor cells lead to cardiac, smooth muscle, and endothelial cell diversification. Cell 2006;127:1151-65.
28. Moretti A, Bellin M, Jung CB, et al. Mouse and human induced pluripotent stem cells as a source for multipotent Isl1+ cardiovascular progenitors. FASEB J 2010;24:700-11.
29. Laugwitz KL, Moretti A, Lam J, et al. Postnatal isl1+ cardioblasts enter fully differentiated cardiomyocyte lineages. Nature 2005;433:647-53. [Erratum, Nature 2007;446:934.]
30. Mummery C, Ward-van Oostwaard D, Doevendans P, et al. Differentiation of human embryonic stem cells to cardiomyocytes: role of coculture with visceral endoderm-like cells. Circulation 2003;107:2733-40.
31. Pan N, Sun J, Lv C, Li H, Ding J. A hydrophobicity-dependent motif responsible for surface expression of cardiac potassium channel. Cell Signal 2009;21:349-55.
32. Wilson AJ, Quinn KV, Graves FM, Bitner-Glindzicz M, Tinker A. Abnormal KCNQ1 trafficking influences disease pathogenesis in hereditary long QT syndromes (LQT1). Cardiovasc Res 2005;67:476-86.
33. Voigt P, Dorner MB, Schaefer M. Characterization of p87PIKAP, a novel regulatory subunit of phosphoinositide 3-kinase gamma that is highly expressed in heart and interacts with PDE3B. J Biol Chem 2006;281:9977-86.
34. Lerche C, Bruhova I, Lerche H, et al. Chromanol 293B binding in KCNQ1 (Kv7.1) channels involves electrostatic interactions with a potassium ion in the selectivity filter. Mol Pharmacol 2007;71:1503-11. [Erratum, Mol Pharmacol 2007;72:796.]
35. Vyas H, Hejlik J, Ackerman MJ. Epinephrine QT stress testing in the evaluation of congenital long-QT syndrome: diagnostic accuracy of the paradoxical QT response. Circulation 2006;113:1385-92.
36. Imredy JP, Penniman JR, Dech SJ, Irving WD, Salata JJ. Modeling of the adrenergic response of the human IKs current (hKCNQ1/hKCNE1) stably expressed in HEK-293 cells. Am J Physiol Heart Circ Physiol 2008;295:H1867-81.
37. Lee G, Papapetrou EP, Kim H, et al. Modelling pathogenesis and treatment of familial dysautonomia using patient-specific iPSCs. Nature 2009;461:402-6.
38. Brunner M, Peng X, Liu GX, et al. Mechanisms of cardiac arrhythmias and sudden death in transgenic rabbits with long QT syndrome. J Clin Invest 2008;118:2246-59.
39. Priori SG, Schwartz PJ, Napolitano C, et al. Risk stratification in the long-QT syndrome. N Engl J Med 2003;348:1866-74.